applied microbiology

Article

Characterization of Gentisate 1,2-Dioxygenase from *Pseudarthrobacter phenanthrenivorans* Sphe3 and Its Stabilization by Immobilization on Nickel-Functionalized Magnetic Nanoparticles

Stamatia Asimakoula [1], Archontoula Giannakopoulou [2], Eirini Lappa [1], Epameinondas Tsagogiannis [1], Alexandra Primikyri [3], Haralambos Stamatis [2] and Anna-Irini Koukkou [1,*]

[1] Laboratory of Biochemistry, Sector of Organic Chemistry and Biochemistry, Department of Chemistry, University of Ioannina, 45110 Ioannina, Greece; s.asimakoula@uoi.gr (S.A.); eirini.lappa@outlook.com (E.L.); e.tsagkogiannis@uoi.gr (E.T.)
[2] Biotechnology Laboratory, Department of Biological Applications and Technologies, University of Ioannina, 45110 Ioannina, Greece; arxontoula.gian@gmail.com (A.G.); hstamati@uoi.gr (H.S.)
[3] Laboratory of Organic Chemistry, Sector of Organic Chemistry and Biochemistry, Department of Chemistry, University of Ioannina, 45110 Ioannina, Greece; a.primikyri@uoi.gr
* Correspondence: akukku@uoi.gr; Tel.: +30-265-100-8371

Citation: Asimakoula, S.; Giannakopoulou, A.; Lappa, E.; Tsagogiannis, E.; Primikyri, A.; Stamatis, H.; Koukkou, A.-I. Characterization of Gentisate 1,2-Dioxygenase from *Pseudarthrobacter phenanthrenivorans* Sphe3 and Its Stabilization by Immobilization on Nickel-Functionalized Magnetic Nanoparticles. *Appl. Microbiol.* **2022**, *2*, 113–132. https://doi.org/10.3390/applmicrobiol2010007

Academic Editor: Pavel Kopel

Received: 24 December 2021
Accepted: 18 January 2022
Published: 21 January 2022

Abstract: The aim of this study was the biochemical and kinetic characterization of the gentisate 1,2-dioxygenase (GDO) from *Pseudarthrobacter phenanthrenivorans* Sphe3 and the development of a nanobiocatalyst by its immobilization on Ni^{2+}-functionalized Fe_3O_4-polydopamine magnetic nanoparticles (Ni^{2+}-PDA-MNPs). This is the first GDO to be immobilized. The gene encoding the GDO was cloned with an N-terminal His-tag and overexpressed in *E. coli*. The nanoparticles showed a high purification efficiency of GDO from crude cell lysates with a maximum activity recovery of 97%. The immobilized enzyme was characterized by Fourier transform infrared spectroscopy (FTIR). The reaction product was identified by ^{1}H NMR. Both free and immobilized GDO exhibited Michaelis–Menten kinetics with K_m values of 25.9 ± 4.4 and 82.5 ± 14.2 μM and V_{max} values of 1.2 ± 0.1 and 0.03 ± 0.002 mM·s^{-1}, respectively. The thermal stability of the immobilized GDO was enhanced at 30 °C, 40 °C, and 50 °C, compared to the free GDO. Stored at −20 °C, immobilized GDO retained more than 60% of its initial activity after 30 d, while the free enzyme completely lost its activity after 10 d. Furthermore, the immobilized nanoparticle–enzyme conjugate retained more than 50% enzyme activity up to the fifth cycle.

Keywords: *Pseudarthrobacter phenanthrenivorans* Sphe3; gentisate 1,2-dioxygenase; His-tagged enzyme; magnetic nanoparticles; oxidoreductase immobilization

1. Introduction

Microorganisms, with their ability to degrade a vast variety of xenobiotic aromatic compounds, under either aerobic or anaerobic conditions, have contributed significantly to the removal of these pollutants from the environment. Although these compounds present a great diversity as far as the number of rings and modifications are concerned, their aerobic biodegradation is invariably funneled through a limited number of dihydroxylated aromatic intermediates, such as catechol, protocatechuate, and gentisate. The subsequent oxygenolytic cleavage of their aromatic ring is catalyzed by enzymes called ring-fission dioxygenases, which are classified as two major groups according to the position of the cleavage of the aromatic ring: intradiols, cleaving the ring between the hydroxyl group (ortho cleavage), and extradiols (Types I and II), cleaving the ring adjacent to the hydroxyl group (meta cleavage). In contrast, non-catecholic intermediates, such as gentisate (a para-

diol), that are subject to extradiol-type cleavage are cleaved by a third type of extradiol dioxygenase (Type III) belonging to the cupin superfamily proteins [1].

Gentisate (2,5-dihydroxybenzoate) is cleaved by gentisate 1,2-dioxygenase (GDO), which catalyzes the ring fission of gentisate between the carboxyl and the proximal hydroxyl group (*para* position) in the aromatic ring, to form maleylpyruvate [2]. All to-date-reported GDOs belong to the bicupin protein superfamily [3–5].

Microbial enzymes that are able to cleave aromatic compounds substituted with a hydroxyl group in the para-position are of industrial interest for the removal of environmental recalcitrant compounds [6].

Aromatic degradation through the gentisate intermediate has been reported in various studies [7–14]. Although several GDOs have been characterized, they are mainly derived from Gram-negative bacteria [6,15–22], whereas there is little information about GDOs from Gram-positive bacteria [4,23,24].

While dioxygenases hold an important role not only in bioremediation of contaminated environments, but also in many technological processes, their potential in biotechnological applications is narrowed not only by the various environmental factors that affect the bioremediation processes, but also by free enzymes' low stability and oxidation susceptibility, resulting in enzymes' deactivation [25]. Moreover, multimeric enzymes' inactivation has been attributed to the dissociation of their subunits in solutions [26–29]. To tackle these challenges, enzymes are being immobilized onto a solid support in order to optimize their performance. The application of a proper immobilization method combined with a suitable immobilization carrier could improve enzymes' operational stability under harsh reaction conditions, their tolerance against harmful agents and inhibitors, and their specificity or selectivity towards various substrates and prevent subunit dissociation for multimeric enzymes. Furthermore, it could even be coupled with enzyme purification, enabling its easy separation and thus reducing the time and cost of any purification and recovery methods required [26,30,31].

Various immobilization supports have been used for the immobilization of dioxygenases, such as sodium alginate [32], single-walled carbon nanotubes [33,34], multi-walled carbon nanotubes [35], Fe_3O_4 nanoparticles [36], and fulvic-acid-activated montmorillonite [37]. Among these supports, magnetic nanoparticles (MNPs) stand out due to their attractive properties, such as their high surface-to-volume ratio and strong magnetization values, which facilitate their separation from the reaction mixture and thus the efficient re-use of the biocatalyst [38]. Until now, notwithstanding the cost of their synthetic route and a typically observed reduced biocatalytic activity [39], magnetic nanoparticles have been widely applied for the immobilization of various classes of enzymes, making them an appealing immobilization support [40]. Specifically, affinity magnetic nanomaterials have recently gained significant attention for simultaneous purification and immobilization of histidine (His)-tagged proteins [41]. This method is based on the principle of immobilized metal affinity chromatography (IMAC), widely used for protein purification and separation. Immobilized metal ions by chelation onto a chromatography resin interact with a His-tag, forming a reversible coordination bond, which allows the separation of histidine-tagged proteins from the untagged ones [42]. The bound molecule can be eluted from the resin by reducing the pH and increasing the ionic strength of the buffer or using EDTA or imidazole. Employing genetic engineering methods allows for the production of tagged enzymes by attaching His residues at a specific position of the protein without altering the enzyme's activity or folding. These tags are usually placed at the N- or C-terminus of the recombinant proteins in the form of a poly-histidine tail. Then, immobilization of the enzyme becomes possible via the interaction of the histidine tail with the nickel ions. It is worth noting, however, that the reversibility of the binding process or the undesired release of the metals to the reaction medium may be a drawback in many cases [43]. The employment of magnetic nanoparticles for protein purification requires fewer purification steps, an obvious advantage when compared to the far more complex and laborious column chromatography methods [44]. Affinity magnetic nanoparticles enable the efficient adsorption

of proteins and can thus facilitate the separation of a target protein in low-concentration samples. Furthermore, their surface functionalization with biopolymer materials, such as polydopamine [41,45], constitutes a simple and economic synthetic method under mild conditions. On the other hand, the widely employed conventional affinity materials and techniques utilize bridging molecules, such as nitrilotriacetic acid (NTA) [46–48], and are characterized as inconvenient and time-consuming processes, usually requiring hazardous reagents. The polydopamine surface coating of the nanoparticles can offer many advantages, such as biocompatibility, water dispersibility, and adhesion properties due to the presence of catechol hydroxyl groups. More specifically, the catechol group could perform chelation with metal ions, such as Ni^{2+}, so that the metal ions could be indirectly immobilized on polydopamine-modified substrates. Until now, nickel-functionalized polydopamine magnetic nanoparticles have been employed for the purification of a His-tagged red fluorescent protein [41], while titanium-functionalized polydopamine magnetic microspheres have been used for the enrichment of biological samples with phosphopeptides [49], suggesting the widespread applications of these immobilization supports.

Pseudarthrobacter phenanthrenivorans Sphe3, a Gram-positive bacterium, is able to catabolize phenanthrene as the sole source of carbon and energy [50]. In silico analysis of the Sphe3 genome revealed a gene on the pASPHE301 plasmid that encodes for a putative gentisate 1,2-dioxygenase (*gtd*A gene).

To the best of our knowledge, no study on the immobilization of gentisate 1,2-dioxygenase from Gram-positive bacteria has yet been published. For the first time, the recombinant gentisate 1,2-dioxygenase from *P. phenanthrenivorans* Sphe3 was cloned, expressed, characterized, and immobilized on the surface of nickel-functionalized Fe_3O_4-polydopamine magnetic nanoparticles (Ni^{2+}-PDA-MNPs). The recombinant enzyme was immobilized on Ni^{+2}-PDA-MNPs while being simultaneously purified utilizing the His-tag affinity with the Ni^{+2}-functionalized surface of the magnetic nanoparticles.

The results of this study should be useful for dioxygenase immobilization on nanomaterials, developing an efficient nanobiocatalytic system utilized in bioremediation processes, aiming to lower the cost and performance of these processes.

2. Materials and Methods

2.1. Materials

Iron (II, III) oxide nanopowder, 50–100 nm particle size (SEM), 97% trace metals basis, and dopamine hydrochloride were purchased from Sigma-Aldrich (St. Louis, MO, USA). Nickel (II) sulfate hexahydrate (*$6H_20O$), 99%, was purchased from Acros Organics. Phenanthrene was purchased from Fluka. Sodium dodecyl sulfate (SDS) was purchased from Honeywell Riedel-de Haën™ (Seelze, Germany), and Bis-acrylamide was bought from Carl Roth (Karlsruhe, Germany). Isopropyl β-d-1-thiogalactopyranoside (IPTG) and protein markers were purchased from New England Biolabs (Ipswich, MA, USA) and Thermo Fisher Scientific (Waltham, MA, USA). All other chemicals used in the present study were bought from Sigma Aldrich (St. Louis, MO, USA).

2.2. Bacterial Strains and Media

P. phenanthrenivorans Sphe3^T (formerly *Arthrobacter phenanthrenivorans* Sphe3 = DSM 1860^T = LMG 23796^T) was isolated from a creosote-polluted area in Epirus, Greece [50]. Sphe3 was grown in M9 minimal medium (MM M9) supplemented with gentisate (5 mM) or phenanthrene (15 mM) as the sole carbon and energy sources, as previously described [51]. *Escherichia coli* DH5a and BL21 (DE3) were cultured in lysogeny broth (LB) medium in the presence of kanamycin (Km), when necessary, for selection.

2.3. Preparation of Sphe3 Cell-Free Extracts

Crude Sphe3 cell-free extracts were prepared as described previously [52]. The protein concentration was determined spectrophotometrically, according to the Bradford

method [53], using the Bio-Rad reagent (Bio-Rad Laboratories, Hercules, CA, USA) and bovine serum albumin (BSA) (Amresco Inc., Solon, OH, USA) as the standard.

2.4. Cloning and Heterologous Expression of the Gentisate 1,2-Dioxygenase Gene

In silico analysis of the Sphe3 genome in the DOE Joint Genome Institute database (JGI—https://img.jgi.doe.gov; accessed on 10 November 2020) revealed an *orf* of 1122 bp that encodes the putative gentisate 1,2-dioxygenase (GDO), located on the indigenous plasmid pASPHE301 and annotated *gtdA*. Genomic DNA was isolated from Sphe3 cells grown on phenanthrene according to the standard JGI (California) protocol for bacterial genomic DNA isolation using cetyltrimethylammonium bromide (CTAB) [54]. *GtdA* gene was amplified by polymerase chain reaction (PCR) in a thermal cycler (PTC-100, v.7.0—MJ Research Inc., Waltham, MA, USA) programmed at 95 °C for 5 min, 35 cycles of 98 °C for 20 s, 66 °C for 15 s, 72 °C for 1 min, and a final elongation step of 72 °C for 5 min, using KAPA HiFi (Roche Diagnostics, Basel, Switzerland) polymerase enzyme and a specific primer pair (forward primer: 5′-AGAGATTCATATGACTGAGAACATC-3′, reverse primer: 5′-AGGAGTTTGGATCCTTGGTG-3′) carrying binding sites for *Nde*I and *Bam*HI (underlined) restriction enzymes. The amplified DNA fragment was purified by NucleoSpin Extract 2 in 1 (Macherey-Nagel GmbH & Co. KG, Dueren, Germany), cloned into the pCR-blunt vector (Invitrogen, Thermo Fischer Scientific, Watham, MA, USA) for nucleotide sequence verification, and subsequently subcloned with *Nde*I/*Bam*HI restriction in the overexpressing vector pET29c$_{(+)}$ (Novagene Co., Ltd., Beijing, China). The recombined pET29c::*gtdA* was used to transform BL21 (DE3) cells for heterologous expression as described elsewhere [51]. Host transformation was carried out either according to Hanahan (for *E. coli* DH5a strain) [55] or according to Chung and Miller (for *E. coli* BL21 (DE3) strain) [56]. Gene nucleotide sequence verification was carried out by VBC Genomics Bioscience Research GmbH (Wien, Germany). Sequence alignments were performed using the program BLAST [57] on the NCBI website, and amino acid sequences that exhibited similarity with GDO were retrieved from protein databases and aligned using CLUSTALW (accessed on 23 November 2021) [58]. To conduct phylogenetic tree and molecular evolutionary analyses, MEGA v.7.0 was used applying the neighbor-joining method [59]. Restriction enzyme digestion, ligation reaction, and agarose, as well as SDS-PAGE electrophoresis were carried out using the standard methodology [60].

2.5. Crude Lysate Preparation and GDO Purification

The abovementioned *E. coli* BL21(DE3)-pET29c$_{(+)}$ host–vector overexpression system was used for the overexpression of the GDO polypeptide, as described elsewhere [51], with the slight modification of harvesting the cells by centrifugation 3 h after the addition of IPTG. For the enzyme purification, cell-free supernatant was applied to a 20 mL HisPrep FF 16/10 column (GE Healthcare, Chicago, IL, USA) using an AKTA FPLC system (GE Healthcare, Chicago, IL, USA), as described before [52].

2.6. Enzyme Assays, Kinetic Measurements

The activity of GDO under standard conditions was estimated spectrophotometrically by measuring the increase in absorbance at 330 nm as described by Feng et al. [15]. The reaction was initiated with the addition of the crude cell-free extract or the recombinant purified GDO solution. One enzyme unit is defined as the amount of enzyme that produces 1 μmol of maleylpyruvate per minute at 25 °C. The kinetic parameters K_m and V_{max} values were determined in a broad concentration range of gentisate substrate varying from 0.003 mM to 3 mM, with EnzFitter (Biosoft) software by nonlinear fitting of the Michaelis–Menten equation. All kinetic values are the means of three separate measurements. The effect of pH in the activity of recombinant GDO was investigated in the pH range of 4 to 12 at room temperature, as described elsewhere [52]. To determine the optimal temperature for the GDO, the above assays were performed in a temperature range of 5 °C to 80 °C in the optimal pH. To study the effect of activation and inhibition by metal ions, the enzyme

was incubated with different concentrations of $FeSO_4 \cdot 7H_2O$/L-ascorbic acid, $CuSO_4 \cdot 5H_2O$, $MnSO_4 \cdot H_2O$, $MgSO_4 \cdot 7H_2O$, and $NiCl_2 \cdot 6H_2O$, as described before [52]. The influence of different chelating agents on the GDO activity was tested by incubating samples of the purified enzyme (1 μM) with concentrations of EDTA up to 20 μM for 120 min at 0 °C and o-phenanthroline up to 30 μM for 180 min at 0 °C in 50 mM Tris-HCl buffer pH 8.0. The enzyme reaction was initiated by adding 0.3 mM gentisate. All enzyme assays were performed at 25 °C using a Shimadzu UV-1201 spectrophotometer (Triad Scientific, Inc., Manasquan, NJ, USA).

2.7. Synthesis of Ni^{2+}-Polydopamine Magnetic Nanoparticles

The Ni^{2+}-PDA-MNPs were synthesized according to Yang et al. [41], with slight modifications. Briefly, in a typical synthesis protocol, 10 mg of commercially available iron oxide magnetic nanoparticles (Fe_3O_4) was dispersed in 10 mL of Tris-HCl buffer (25 mM, pH 8.0) for 30 min in an ultrasonic bath. Subsequently, 10 mg of dopamine hydrochloride was added to the above dispersion and mixed under constant magnet stirring (750 rpm) for 12 h at 25 °C. The polydopamine functionalized magnetic nanoparticles were then gathered through magnetization and washed several times with water. Afterwards, the nanoparticles were added to 10 mL of 100 mM $NiSO_4$ solution and mixed under constant stirring (750 rpm) for 2 h at 25 °C. Finally, the freshly prepared Ni^{2+}-PDA-MNPs were collected with the use of an external magnet, washed twice, and stored in deionized water for further use.

2.8. Selective Immobilization of the Recombinant GDO on Ni^{2+}-PDA-MNPs

For the selective immobilization of recombinant gentisate 1,2-dioxygenase on Ni^{2+}-PDA-MNPs, 100 μL of freshly prepared magnetic nanoparticles (2 mg/mL), ultrasonically dispersed in Tris-HCl buffer (50 mM, pH 8.0), was added to 900 μL of cell-free extract containing the recombinant GDO (total protein concentration of 4 mg/mL). Then, the mixture was incubated at room temperature for 30 min, under constant magnetic stirring (650 rpm). After incubation, the nanobiocatalyst was separated from the reaction mixture with the use of an external magnet, washed twice with buffer, and stored at −20 °C for further use. Several parameters affecting the immobilization yield such as the ratio of Ni^{2+}-PDA-MNPs to total enzyme mass (1:2, 3:2, 4:2, and 1:10) and the incubation time (30 min and 120 min) were examined and optimized, in order to attain the maximum immobilization yield. The immobilization percentage was determined by measuring the activity in the stock-free enzyme solution and also through the determination of the remaining activity in the supernatant and in the immobilization solution after the immobilization procedure, as suggested elsewhere [61,62].

2.9. Characterization of the Nanobiocatalyst

2.9.1. Fourier Transform Infrared Spectroscopy

In order to confirm the characteristic functional peaks of the nanobiocatalyst, FTIR spectroscopy was performed through an FTIR-8400 infrared spectrometer (Shimadzu, Tokyo, Japan) equipped with a deuterated triglycine sulfate (DTGS) detector. All spectra were recorded within the 400–4000 cm^{-1} range and an average of 32 scans.

2.9.2. Identification of Nanobiocatalyst Reaction Product

There was 40 μL of nanobiocatalyst used in a 1 mL reaction with gentisate as the substrate at a final concentration of 0.3 mM. The reaction was kept at 4 °C for 12 h, and after centrifugation, the supernatant was transferred to a 5 mm NMR tube in 50 mM Tris buffer pH 8.0, 90% H_2O, and 10% D_2O. The ^{1}HNMR experiment was performed on a Bruker AV500 spectrometer (Bruker Biospin, Rheinstetten, Germany) at 298 K using the Topsin 3.2 suite. The water suppression was achieved by the use of an excitation sculpting pulse sequence (zgesgp).

2.9.3. Determination of Apparent Kinetic Parameters

The apparent kinetic constants (K_m, V_{max}) of the immobilized biocatalyst were determined by measuring the initial reaction rates at varying concentrations of the gentisate substrate at 25 °C as described above. The concentrations of gentisate ranged from 0.01 mM to 0.3 mM. The apparent Michaelis–Menten constant (K_m) and maximum velocity (V_{max}) were calculated from non-linear regression fitting of the initial reaction rates corresponding to different substrate concentrations by the EnzFitter (Biosoft) software.

2.9.4. Thermal Stability of Free and Immobilized Biocatalyst

Thermal stability studies of the free and immobilized biocatalyst were performed by incubating each form of the enzyme in Tris-HCl buffer (50 mM, pH 8.0) at 30 °C, 40 °C, and 50 °C for 24 h. The remaining activity of the free and immobilized biocatalyst was determined at different time intervals (1 h, 3 h, 6 h, 9 h, and 24 h) through the activity assays, as described above. All experiments were carried out in triplicate.

2.9.5. Storage Stability Studies

The storage stability of the free and immobilized form of the biocatalyst was estimated during storage at −20 °C. The activity of each sample was evaluated at standard day intervals for a total of 30 d. The activity of each enzyme after standard day intervals was estimated in terms of residual activity using the respective assay by considering the activity of the first day to be 100%.

2.9.6. Reusability Studies of Immobilized Enzyme

The reusability of the immobilized nanobiocatalyst was determined through the completion of continuous batch reactions for the cleavage of gentisate to form maleylpyruvate. Each reaction cycle was carried out for 10 min in Tris-HCl buffer solution (50 mM, pH 8.0). After each cycle, the nanobiocatalyst was separated from the reaction mixture through magnetization, washed efficiently with Tris-HCl buffer solution (50 mM, pH 8.0), and then, re-suspended in fresh substrate solution to initiate a new reaction cycle. The process was repeated for 10 successive cycles. The activity of the nanobiocatalyst after each cycle was assessed by means of residual activity. The activity of the first cycle was considered as 100%.

3. Results and Discussion

3.1. Phylogenetic Analysis, Cloning, and Overexpression

The predicted protein product of the 1122 bp gentisate 1,2-dioxygenase gene (*gtdA*) from *P. phenanthrenivorans* Sphe3 shared 92.7% sequence identity at the amino acid level with gentisate 1,2-dioxygenase (GDO) of *Arthrobacter* sp. (strain FB24). Based on a phylogenetic analysis of 18 GDO amino acid sequences with Molecular Evolutionary Genetics Analysis software v.7.0 (MEGA7) [59] using the neighbor-joining method [63], it was found that Sphe3-GDO clustered with similar dioxygenases from other Gram-positive bacteria. In particular, Sphe3-GDO was most closely related to the gentisate 1,2-dioxygenase from *Arthrobacter oryzae* with *Arthrobacter* sp. FB24, *Arthrobacter globiformis* NBRC 12137, and *Arthrobacter* sp. P2b, completing the brunch clustering (Figure 1).

The *gtdA* from *P. phenanthrenivorans* Sphe3 was amplified by PCR, cloned, and expressed as a His-tagged protein in *E. coli* BL21 (DE3) using the pET29c$_{(+)}$ overexpression vector. The recombinant GDO resulted in a protein band of ~41 kDa, as determined by sodium dodecyl sulfate-polyacrylamide gel electrophoresis (SDS-PAGE) (Figure S1), corresponding well to the predicted, by the in silico analysis, Mw of 41.45 kDa.

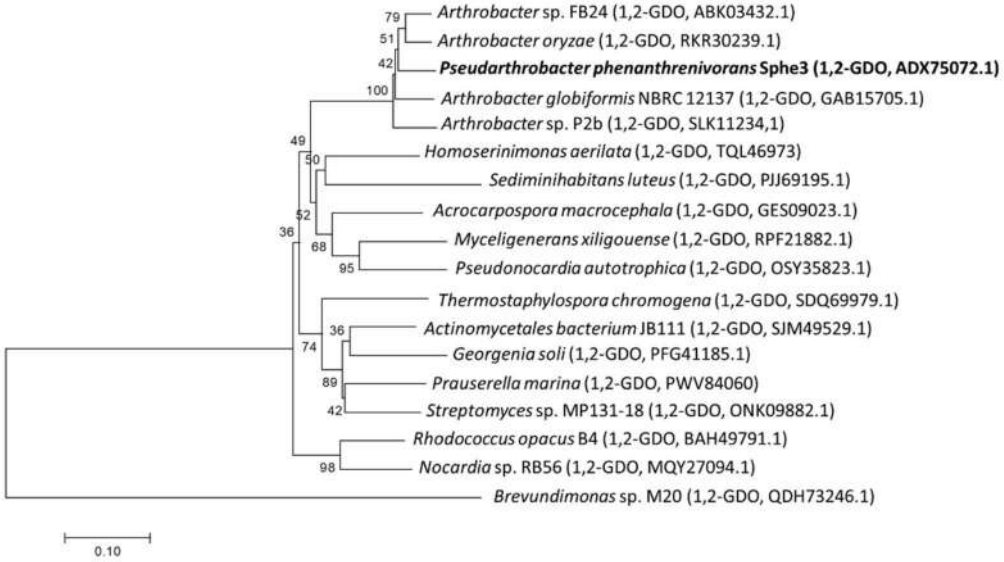

Figure 1. Phylogenetic tree of Sphe3 1,2-GDO and other Gram-positive 1,2-GDO dioxygenases. The dioxygenases used for the construction of the phylogenetic tree presented >70% identity with GDO. 1,2-GDO from the Gram-negative *Brevundimonas* sp. M20 (QDH73246.1), showing 38% identity with Sphe3 1,2-GDO, served as the outer brunch. The tree was constructed with the neighbor-joining algorithm. The percentage of replicate trees in which the associated dioxygenases clustered together in the bootstrap test (500 replicates) is shown next to the branches. The scale bar indicates the number of substitutions per nucleotide position. Accession numbers are in parentheses. 1,2-GDO: gentisate 1,2-dioxygenase.

3.2. Enzyme Activity Assay and Characteristics of Purified GDO

The cell-free extract of BL21 (DE3) cells showed a specific activity of 1.7 U·mg^{-1} protein against gentisate, whereas the purified enzyme, which was at least 95% homogeneous, exhibited specific activity of 10.7 U·mg^{-1} protein. Purification of GDO was achieved by a HisPrep FF 16/10 column, prepacked with precharged Ni Sepharose 6 Fast Flow, using a step gradient as described in the "Materials and Methods". The fractions of the overexpressed protein were eluted at ~150 mM imidazole, pooled, and assayed for activity.

The purified GDO displayed Michaelis–Menten kinetics with an apparent K_m 25.9 ± 4.4 μM and V_{max} 1.2 ± 0.1 mM·s^{-1} as estimated at 25 °C. The K_m value of GDO for gentisate is lower than or similar to values reported for gentisate 1,2-dioxygenases from other organisms (85 μM, *Pseudomonas testosteroni* and 74 μM, *Pseudomonas acidovorans* [16]; 15 μM, *Sphingomonas* sp. RW5 [18]; 92 μM, *Pseudomonas alcaligenes* NCIB 9867 and 143 μM, *Pseudomonas putida* NCIB 9869 [15]; 31 μM and 10 μM, *Polaromonas naphthalenivorans* CJ2 [20]; 130 μM, *Corynebacterium glutamicum* [23]), revealing a high affinity with gentisate as the substrate. The turnover number of GDO was also similar to the values reported for other organisms [18,19], exhibiting a K_{cat} value of 60 ± 3.4 s^{-1}, whereas the K_{cat}/K_m value was 231.6 × 10^4 s^{-1}·M^{-1}.

The purified enzyme was highly unstable as it lost 75% of its initial specific activity when it was stored at 4 °C for 48 h. Similar results have also been reported previously for GDOs purified from *Klebsiella pneumoniae* M5al, *Sphingomonas* sp. strain RW5, *Pseudomonas alcaligenes* NCIB 9867, *Pseudomonas putida* NCIB 9869 and *Ralstonia solanacearum* GMI 1000 [15,18,22,64]. The enzyme could not be stabilized by the addition of glycerol (10% *v*/*v*), ethanol (10% *v*/*v*), and DMSO (1% or 10%, *v*/*v*). Moreover, the addition of Fe^{2+} increased the enzyme activity by 3.7-fold. In fact, when the purified enzyme was incubated in the presence of the 0.2 mM $FeSO_4$/L-ascorbic acid solution for 30 min at 0 °C, its specific activity reached at 39.6 U·mg^{-1} protein. This suggests that the active site Fe^{2+} is probably lost during the purification process and exogenously supplemented Fe^{2+} activated the purified enzyme [65,66]. Ferrous iron is the catalytically competent metal cofactor as has

been established by biochemical studies [64,67]. Similar results have also been reported previously, presenting an increased GDO activity by 160% for *P. alcaligenes* NCIMB 986710, by 115% for *E. coli* O157:H7, and by 34% for the *Martelella* strain AD-3 [6,68,69]. Ferrous biding is also important for the GDO activity of *Silicibacter pomeroyi*, in which both the N and C domain maintain the histidine triad and bind with Fe^{2+}, unusually with other GDOs where the N-terminal cupin domain binds metal and maintains the active site [4,21].

Incubation with various concentrations of Cu^{2+}, Mn^{2+}, Mg^{2+}, and Ni^{2+} for 30 min exhibited inhibitory effects, leading to an enzymatic activity loss of 47%, 14%, 5%, and 43%, respectively. The addition of Cu^{2+} and Mn^{2+} could also inactivate the GDO from *Pseudomonas alcaligenes* NCIB 9867, *Pseudomonas putida* NCIB 9869, and *Ralstonia solanacearum* GMI 1000 [15,22], whereas Cu^{2+} and Mn^{2+} activated GDO from the *Martelella* strain AD-3 [69]. Moreover, the incubation of GDO with metal-chelating agents led to a significant reduction or even complete inhibition of the enzyme's activity. Specifically, incubation with different concentrations of EDTA for 180 min reduced GDO's activity, while incubation with o-phenanthroline for 120 min attained to inhibit the enzyme's activity (Table 1).

Table 1. Metal-chelating agents used in various concentrations for incubation with purified GDO.

Concentration (μM)	Relative Activity (%)	
	EDTA	o-Phenanthroline
0	100	100
5	95	41
10	50	10
15	48	4
20	46	0
25	44	N/A
30	40	N/A

These findings for the herein studied gentisate 1,2-dioxygenase are in compliance with studies about dioxygenases possessing iron Fe^{2+} at their active sites being sensitive to chelators [15,65,70,71].

3.3. Immobilization of Recombinant Gentisate 1,2-Dioxygenase

The magnetic nanobiocatalyst was prepared by cross-linking the overexpressed His-tagged gentisate 1,2-dioxygenase without purification from the cell-free crude extract onto magnetic nanoparticles (MNPs) employing the His-tag affinity of the recombinant enzyme to the Ni^{2+}-functionalized surface of the MNPs (Figure 2).

One-step immobilization and purification methods have been applied before for a His-tagged transaminase [41], a histidine-tagged green fluorescent protein [72], an extracellular His-tagged *Thermomyces lanuginosus* lipase [73], and even for the co-immobilization of two components of hydroxylase monooxygenase that were employed to construct a bi-enzymatic catalytic system [46]. Moreover, Zhou et al. studied the selective purification and immobilization of a His-tagged recombinant glucose dehydrogenase onto $NiFe_2O_4$ magnetic nanoparticles in a one-step procedure [74]. The abovementioned methodology allowed for the selective purification of the recombinant GDO through immobilization on the nanocarriers.

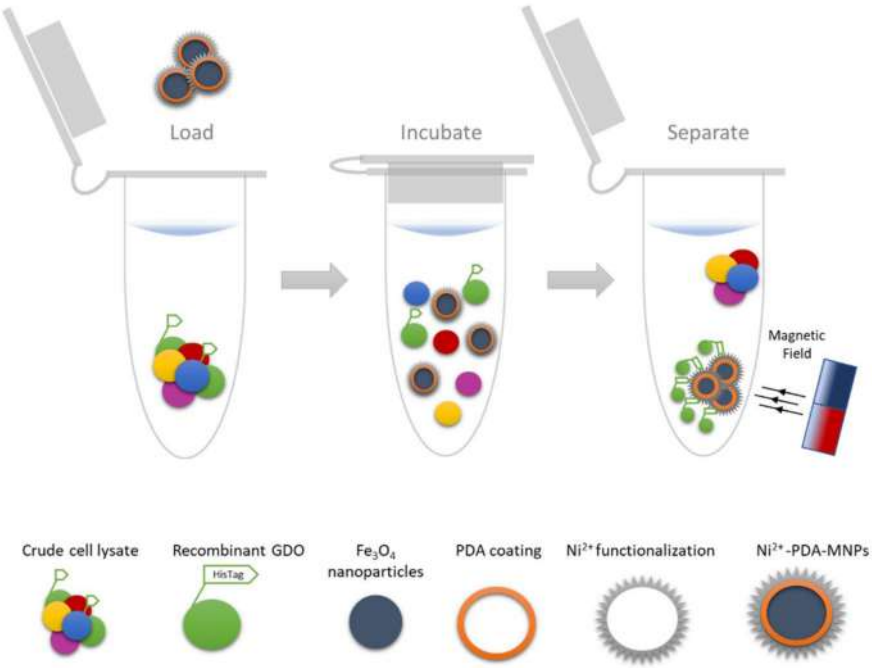

Figure 2. Scheme of the one-step immobilization and purification of His-tagged GDO on Ni^{2+}-PDA-Fe_2O_4 magnetic nanoparticles.

In order to achieve the maximum enzyme loading onto the surface of the Ni^{2+}-functionalized MNPs, several parameters, such as the incubation time and the MNPs-to-enzyme-mass ratio, were examined and optimized. Regarding the incubation time, 30 min and 120 min were examined, revealing that an incubation time of 30 min seems to favor the enzyme's immobilization yield (Figure S2). Concerning the mass ratio of Ni^{2+}-PDA-MNPs to the total enzyme amount, several mass ratios (1:2, 3:2, 4:2, and 1:10) were tested. The enzyme's activity recovery does not seem to be significantly affected at different mass ratios (Figure 3). However, the lowest activity recovery was observed at the highest mass ratio of 1:10, probably due to the insufficient available surface area of the nanocarrier to load the large amount of enzyme, resulting in decreased activity recovery [75,76]. The increase of the amount of MNPs led to an increase of the enzyme's activity recovery, and specifically, the maximum activity recovery was observed at the ratio of 4:2 (Figure 3).

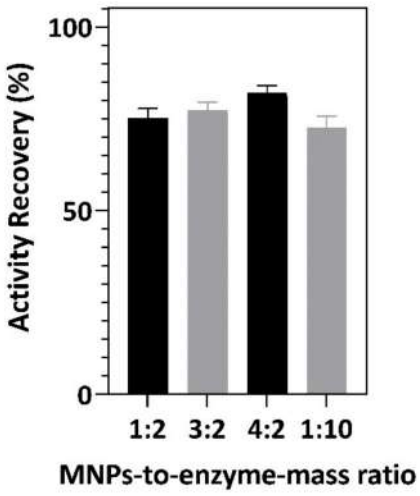

Figure 3. Immobilization parameters optimization in relation to magnetic nanoparticles-to-enzyme-mass ratio.

This could probably be attributed to the fact that a higher amount of nanoparticles could be beneficial to capture the His-tagged protein from the cell-free lysate. Therefore, based on the results presented above, the optimum parameters for the immobilization of recombinant GDO on Ni^{2+}-PDA-MNPs comprised a 30 min incubation time and 4:2 nanoparticles-to-enzyme-mass ratio. Under these conditions, the maximum activity recovery was 97%.

3.4. Characterization of the Nanobiocatalyst

3.4.1. Fourier Transform Infrared Spectroscopy

The successful binding of GDO on the prepared magnetic nanoparticles was confirmed with FTIR analysis. Figure 4 shows the FTIR spectra for the magnetic nanoparticles, the cell-free crude extract from *E. coli* BL21/pET29c::*gtd*A, and the GDO-bound Fe_3O_4. The specific amide group absorptions, amide I, II, and III, in the region 1200–1700 cm^{-1} suggest the presence of a H–N–C–O unit [77,78]. The obvious peak at 1631 cm^{-1} on the crude extract is also present on the nanoparticles containing the immobilized GDO, therefore suggesting the attachment of the enzyme to Fe_3O_4 nanoparticles. This particular peak, which is attributed to C=O stretching vibrations of the enzymes corresponds to the amide I band. The FTIR spectrum of the immobilized GDO is also characterized by a distinct peak at 1551 cm^{-1}, which is due to the C–N stretching and N–H bending vibrations corresponding to the amide II band.

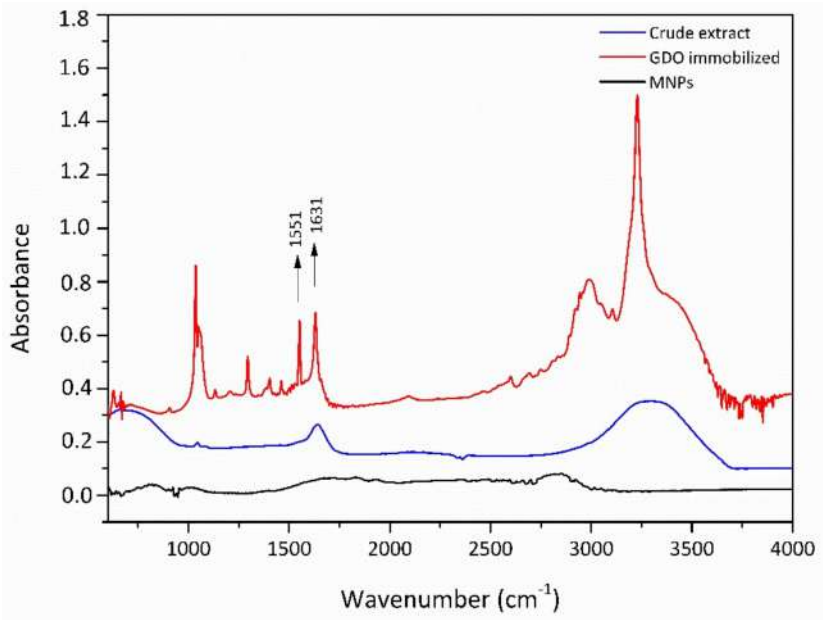

Figure 4. Fourier transform infrared (FTIR) spectra of MNPs (black), cell-free crude extract (blue), and immobilized GDO (red).

The immobilized GDO was separated with the assistance of a magnetic field and washed twice with Tris-HCl buffer. The immobilized GDO was eluted from the Ni^{2+}-PDA-MNPs with 0.5 mL elution buffer containing imidazole at a final concentration of 500 mM. Finally, the collected samples were analyzed by SDS-PAGE to verify the binding specificity between the His-tagged GDO and MNPs. The target protein in the cell lysates was significantly reduced in the supernatant of the immobilization reaction after mixing with the MNPs, while no significant changes in other protein bands were observed (Figure 5, Lane 2). After elution by imidazole, the eluent appeared as a single protein band at 41 kDa, as seen in Figure 5, Lane 3.

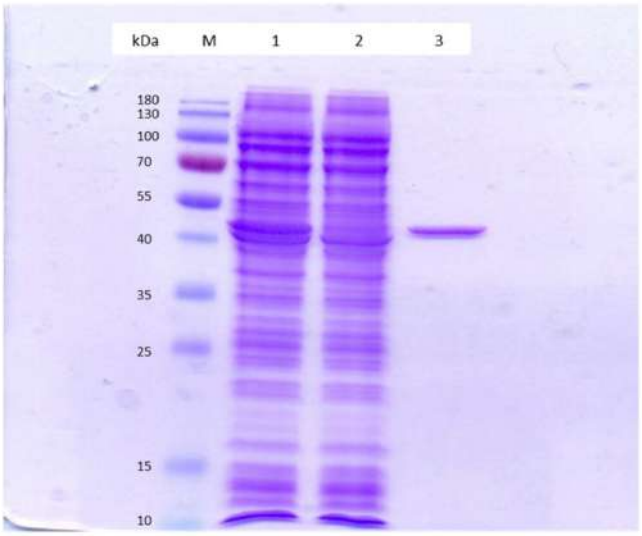

Figure 5. SDS-PAGE protein analysis for the purification of immobilized GDO from the nanobiocatalyst. Lane M, protein molecular mass marker in kDa; Lane 1, cell-free crude extract from *E. coli* BL21 (DE3)-pET29c::*gtdA*; Lane 2, supernatant from the immobilization reaction; Lane 3, eluted GDO protein (41 kDa) with 500 mM imidazole elution buffer.

The abovementioned data combined verify that the His-tagged GDO could bind specifically to Ni^{2+}-PDA-MNPs, proving that the functionalized nanoparticles can effectively be used for the separation and purification of His-tagged protein.

3.4.2. Identification of the Nanobiocatalyst Reaction Product

The ^{1}HNMR spectrum was recorded after the reaction took place for 12 h at 4 °C. The assignment of the gentisate proton NMR resonances is in accordance with literature [79]. The ^{1}HNMR resonances of the maleylpyruvate product are presented for the first time to our knowledge. The peak at 5.75 ppm was attributed to proton H3 and the quartet peak at 6.21 ppm to protons H5 and H6, which overlapped (Figure 6). The substrate and the product ration after 12 h of reaction was 1:1.

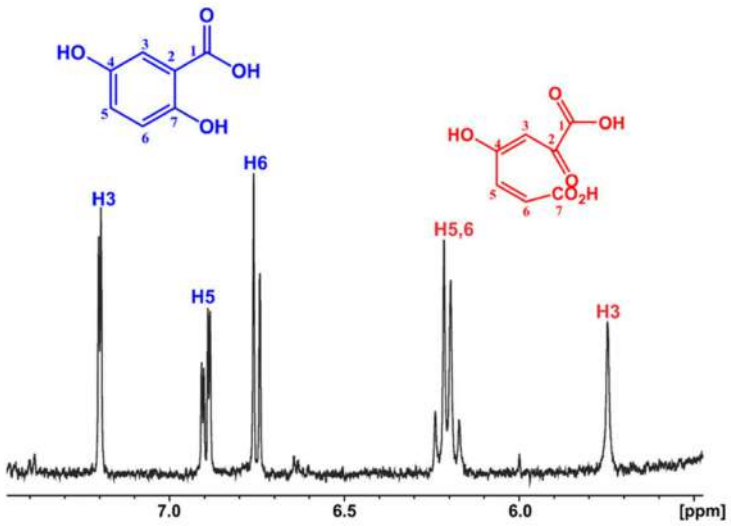

Figure 6. ^{1}H NMR spectrum of the gentisate (blue) biotransformation product, maleylpyruvate (red) in 50 mM Tris buffer 90% H_2O and 10% D_2O. (number of scans = 64, acquisition time = 4 s, relaxation delay = 1.5 s, total experimental time = 6 min 22 s).

3.4.3. Comparison of Free and Immobilized GDO Kinetic Parameters

The intrinsic (for the free form of the enzyme) and apparent (for the immobilized enzyme) Michaelis–Menten constants were determined through the nonlinear regression fitting of the initial reaction rates, with respect to varying gentisate concentrations. As shown in Table 2, the apparent K_m value of the immobilized form of GDO is higher than that of the free enzyme.

Table 2. Apparent kinetic constants of free and immobilized GDO.

Enzyme	K_m (μM)	V_{max} ($mM \cdot s^{-1}$)
GDO free form	25.9 ± 4.4	1.2 ± 0.1
GDO immobilized	82.5 ± 14.2	0.03 ± 0.002

An increase in the K_m value is typically observed after immobilization. This increase could probably be attributed to conformational changes on the protein molecule after immobilization that reduce its flexibility and, thus, restrict the diffusion of the substrate to the active site of the enzyme. These results are in agreement with previous studies that reported an increase in the K_m value after immobilization [40]. Furthermore, Jiao et al., recently reported an increase in the K_m value after immobilizing a recombinant carbonic anhydrase II from human (hCA II) on Ni-based metal-organic framework nanorods [80]. Moreover, the apparent V_{max} value was significantly decreased after immobilization, indicating lower enzymatic reaction rates of the substrate, probably due to the steric hindrance of the support after immobilization. Lower V_{max} values after enzyme immobilization were similarly reported before [33,81]. In another study, Zhou et al. reported about a 6.7-fold decrease in the V_{max} value after the immobilization of a His-tagged recombinant glucose dehydrogenase (GluDH) on $NiFe_2O_4$ magnetic nanoparticles [74].

3.5. Stability of Free and Immobilized Biocatalyst

3.5.1. pH and Temperature Stability Studies

The activity of free and immobilized gentisate 1,2-dioxygenase was measured at different pH values. Free and immobilized GDO were found to be active within pH 5.0 and 10.5, while at pH 4.5 and pH 11.0 both forms of the enzyme completely lost their activity. The pH range 7–12 was preferred for the comparison of the free and immobilized enzymes, due to the fact that the histidine residues of the His-tag are protonated in acidic environments, resulting in the decomposition of the His-tag-Ni^{2+} complex. As shown in Figure 7, the activity profiles for the free and immobilized GDO were different and the pH value of optimum activity shifted from 8.0, for the free enzyme, to 9.0, for the immobilized enzyme. Such a slight shift in pH towards the alkali region after immobilization on nanocarriers has been reported before for other dioxygenases. Di Nardo et al. [82] observed a shift in pH from 8.5 to 9.5 after immobilizing catechol 1,2-dioxygenase on nanosponges. Moreover, Suma et al. found that after immobilizing hydroxyquinol 1,2-dioxygenase onto single-walled carbon nanotubes, the pH value for the optimal activity changed to 8.0 in comparison to pH 7.0 for the free enzyme [33]. According to Das et al., the immobilization of protocatechuate 3,4-dioxygenase onto functionalized multi-walled carbon nanotubes showed an improvement of activity against a higher alkali region, indicating higher stability compared to its free counterpart [35].

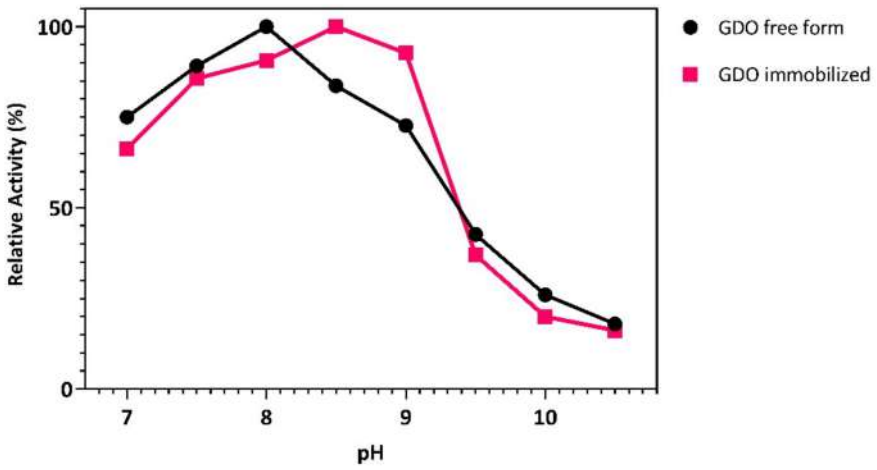

Figure 7. Effect of pH on the activity of GDO in its free form (black) and after immobilization (colored). The activities at the optimal pH were set to 100% for each case.

The effect of temperature on GDO activity was evaluated in 50 mM Tris-HCl buffer (pH 8.0) at temperatures ranging between 5 °C and 80 °C for both the free and immobilized enzyme. The free enzyme was found to be active in the abovementioned temperature range with an optimum activity at 50 °C, while its activity was remarkably reduced to 38% and 8% relative activity at 5 °C and 80 °C, respectively. No significant differences were observed when the effect of temperature on the immobilized enzyme was studied (Figure S3), demonstrating that the optimum temperature for both free and immobilized enzymes was 50 °C, thereafter declining with further increases in temperature. This finding is in agreement with a previous study reporting no change in the temperature optima after immobilization onto functionalized magnetic nanoparticles for b-glucosidase (BGL) from *Aspergillus niger* [83].

3.5.2. Thermal Stability Studies

Among the great advantages of immobilizing an enzyme onto a solid support is to expand its lifespan at extreme conditions, as well as to develop biocatalysts with enhanced catalytic characteristics, widening their industrial applications. An increase in the thermal stability of the biocatalyst after immobilization consists a competitive advantage, suggesting improved resistance to unfolding during long-term incubation [38]. In order to study the influence of temperature on the thermal stability of the biocatalyst, the free form of GDO, as well as the immobilized enzyme were incubated at different temperatures (30 °C, 40 °C, and 50 °C) and their stability was investigated by measuring the residual activity at standard time intervals. A similar trend appeared for both forms of GDO with the residual activity decreasing as the temperature increases. However, the immobilized enzyme was significantly more stable than the free enzyme at all temperatures (Figure 8), retaining more than 30% of its initial activity even after 24 h of incubation at all tested temperatures, while the free enzyme lost almost completely its initial activity after 9 h at 30 °C and 40 °C. At 50 °C, no activity could be measured for the free form of the enzyme after 6 h of incubation. Similar results, suggesting enhanced thermal stability, have been reported for the immobilization of His-tagged β-glucosidase via Fe_3O_4-PMG core–shell magnetic nanoparticles [84].

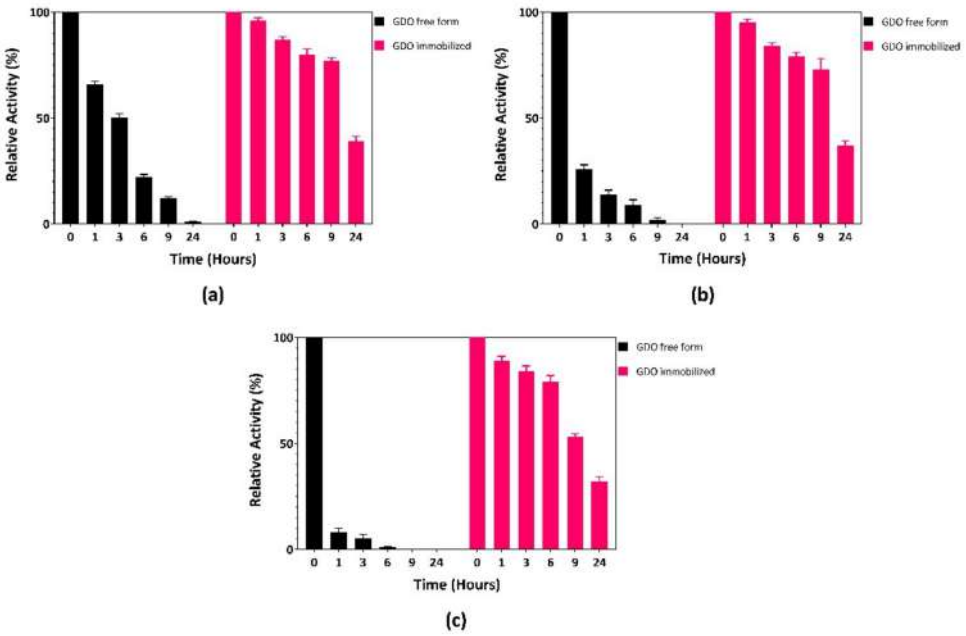

Figure 8. Thermal stability studies of GDO in its free form (black) and GDO immobilized (colored) during storage at 30 °C (**a**), 40 °C (**b**), and 50 °C (**c**) for various timepoints up to 24 h. The activity of the first timepoint was set to 100%.

More specifically, the free enzyme completely lost its activity at 60 °C, while the immobilized one retained almost 75% of its initial activity, suggesting that the binding of His-tagged enzyme onto the nickel-modified magnetic nanoparticles could possibly protect the enzyme's active site, avoiding heat denaturation. Additionally, since the majority of known GDOs from Gram-negative and Gram-positive bacteria are tetramers [4,6], it is worth noting that the His-tag-Ni^{2+} complex may have caused the protein to become less prone to conformational change, protecting the enzyme from thermal denaturation. As reported in the Introduction, the first step of the inactivation of some multimeric enzymes is the enzyme subunit dissociation induced by heat [26,27]. The application of nickel-functionalized polydopamine nanoparticles for the immobilization of a His-tagged ω-transaminase also significantly improved the enzyme's thermal stability, as well as pH tolerance [41]. Das et al. observed a similar behavior regarding the thermal stability of the immobilized protocatechuate 3,4-dioxygenase onto functionalized multi-walled carbon nanotubes [35]. Furthermore, a three-times higher (when compared with the free enzyme) thermal stability of catechol 1,2-dioxygenase immobilized on a nanosponge was reported by Di Nardo et al. [82]. Our results, as well as the studies mentioned suggest that the immobilization of His-tagged enzymes through affinity immobilization methods could lead to the development of robust biocatalysts, exhibiting great stability against denaturation in high-temperature environments. Especially, when concerning the dioxygenase enzymes that are typically characterized by low thermal stability, the immobilization onto appropriate supports constitutes one of the most effective ways to enhance their stability and, thus, broaden their applications.

3.5.3. Storage Stability Studies

Enzyme inactivation or protein denaturing, environmental changes, active-site poisoning or blockage, and a decrease in the enzyme–substrate complex formation result in enzyme activity loss and low stability, rendering the direct application of enzymes in bioremediation processes ineffective [85,86]. The instability of dioxygenases for long time periods seems to be a common issue among these types of enzymes [18,64]. For this reason, the storage stability remains a crucial parameter when concerning such enzymes. The storage stability of the free and immobilized biocatalyst was tested, and the results are

presented in Figure 9. The purified GDO was found to be extremely unstable in 50 mM Tris-HCl buffer. After 48 h of storage at 4 °C in Tris-HCl buffer, its activity decreased to 25% of the original activity (data not shown). No activity was detected for the enzyme after 96 h of storage at 4 °C.

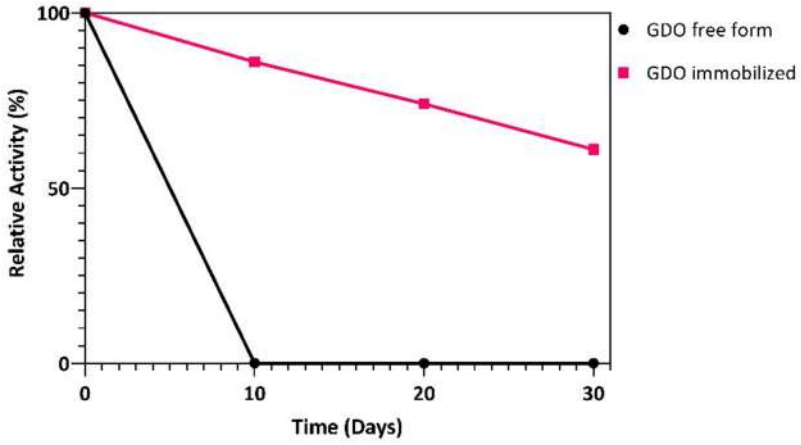

Figure 9. Storage stability study of GDO in its free form (black) and after immobilization (colored) during storage at −20 °C for 1 month. The activity of the first day was set to 100%.

The storage stability for the immobilized magnetic complex was studied for a total of 30 d during storage at −20 °C in an aqueous buffer solution (Tris-HCl 50 mM, pH 8.0). As shown in Figure 9, the immobilized GDO retained more than 60% of its initial activity after 30 d, while no residual activity was detected upon the same storage conditions for the free form of the enzyme. This result is in agreement with other studies where immobilization of enzymes extends their storage stability [87,88]. For example, during 10 d of storage, the His-tagged carbonic anhydrase II immobilized on Ni-based metal-organic framework nanorods maintained 40% activity, while the free enzyme lost 91% of its initial activity [80]. These results indicate that the immobilization of His-tagged enzymes on Ni-modified supports could provide stability and mechanical protection towards denaturation against prolonged storage.

3.5.4. Reusability Studies of Immobilized Enzyme

One of the greatest advantages enzyme immobilization offers is reusability, especially when magnetic nanoparticles are applied as the nanocarrier. To study the nanobiocatalyst's reusability, the immobilized enzyme was recovered by magnetic separation from the reaction mixture after each batch reaction, washed thoroughly with buffer, and added to fresh substrate solution for the next batches. As shown in Figure 10, the immobilized biocatalyst could be efficiently reused for five reaction cycles. It can be observed from Figure 10 that the activity of the immobilized GDO decreased with the increase of the recycling number. However, more than 50% of the enzyme's initial activity was retained for five cycles of consecutive use. GDO's relative activity, though decreased, was also detectable for five more cycles (data not shown). This loss in activity could be probably attributed to any mechanical damage of the biocatalyst during the recycling process along with product inhibition, as has been previously reported [76].

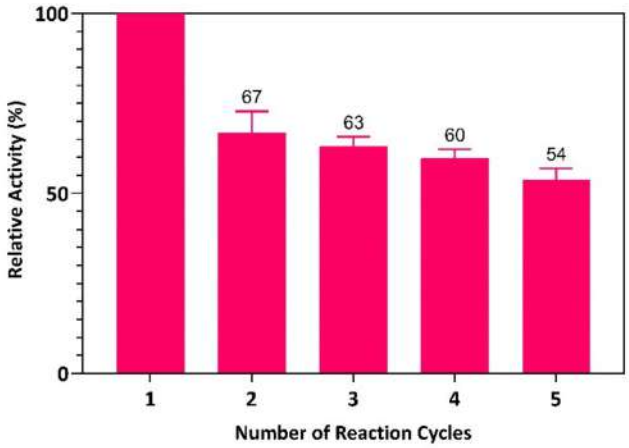

Figure 10. Reusability study of the immobilized GDO. The activity of the first cycle was set to 100%. The number above each bar in the scheme represents the immobilized enzyme's relative activity, expressed in percentage units, for each cycle.

Although no reusability data of gentisate 1,2-dioxygenase have been reported by any other study so far, similar data can be comparable to other enzymes immobilized on various supports [35,46,84,89,90]. Consequently, our study demonstrates that GDO immobilized on MNPs can be efficiently reused, which would be of great benefit for practical applications.

4. Conclusions

This is the first report on the biochemical and kinetic characterization of a gentisate 1,2-dioxygease in the genus *Arthrobacter*. Gentisate 1,2-dioxygenase from *P. phenanthrenivorans* Sphe3 (GDO) was overexpressed, purified and characterized for its biochemical and kinetic properties. The recombinant GDO enzyme was immobilized onto nickel-functionalized polydopamine-coated magnetic nanoparticles (Ni^{2+}-PDA-MNPs). In summary, a simple and efficient method for the immobilization of the recombinant GDO without prepurification was applied by using iron oxide Ni^{2+}-PDA-MNPs to simultaneously purify and immobilize the His-tagged enzyme directly from the cell-free culture supernatant via affinity binding. The developed nanobiocatalyst was characterized by Fourier transform infrared spectroscopy (FTIR), and its reaction product was identified by ^{1}H NMR. The optimal conditions for the immobilization of gentisate 1,2-dioxygenase onto Ni^{2+}-PDA-MNPs were found to be 30 min of incubation time and a 4:2 nanoparticles-to-enzyme-mass ratio, yielding an activity recovery of 97%. Biochemical parameters such as kinetic constants and thermal stability were also evaluated. The analysis of the apparent kinetic constants revealed an increase in the K_m value followed by a decrease in the V_{max} value after immobilization compared with the free form of the enzyme. In addition, due to the magnetic core of the Ni^{2+}-PDA-MNPs, the biocatalyst could be efficiently separated from the reaction through magnetization, facilitating its reuse, thus retaining significant enzyme activity for up to five consecutive reaction cycles. Furthermore, compared with the free enzyme, the immobilized biocatalyst exhibited better thermal stability in a wide range of temperatures. The immobilized GDO retained more than 60% of its initial activity after 30 d of storage at −20 °C compared to the extremely unstable free enzyme. The numerous advantages of immobilization through His-tag affinity promote high yields and efficiency of the total process, suggesting the good potentials this method holds for the design of novel biocatalysts for a wide range of applications.

Supplementary Materials: The following supporting information can be downloaded at: https://www.mdpi.com/article/10.3390/applmicrobiol2010007/s1, Figure S1: SDS-PAGE protein analysis; Figure S2: Immobilization parameters' optimization in relation to incubation time; Figure S3: Effect of temperature on the activity of GDO.

Author Contributions: A.-I.K. conceived of and supervised the study; H.S. contributed to the overall design of the immobilization experiments and the results' interpretation; E.L. and E.T. designed and performed the purification and characterization of GDO; S.A. performed the overexpression and immobilization of GDO, biocatalytic experiments, and results' interpretation; S.A. and A.G. performed the FTIR experiments and contributed to the result analysis; A.P. designed and performed the NMR experiments; S.A., A.G. and A.P. analyzed the data; A.-I.K., S.A., A.G., E.T., A.P. and H.S. wrote the manuscript. A.-I.K. and H.S. made manuscript revisions. All authors have read and agreed to the published version of the manuscript.

Funding: The research work was supported by the Hellenic Foundation for Research and Innovation (HFRI), under the HFRI PhD Fellowship grant (Fellowship Number 1535) attributed to S.A.

Data Availability Statement: All data generated or analyzed during this study are included in this published article (and its Supplementary Materials).

Conflicts of Interest: The authors declare no conflict of interest. HFRI had no involvement in study design; in the collection, analysis, or interpretation of the data; in the writing of the manuscript; nor in the decision to submit the article for publication.

References

1. Vaillancourt, F.H.; Bolin, J.T.; Eltis, L.D. The Ins and Outs of Ring-Cleaving Dioxygenases. *Crit. Rev. Biochem. Mol. Biol.* **2006**, *41*, 241–267. [CrossRef] [PubMed]
2. Lack, L. The Enzymic Oxidation of Gentisic Acid. *Biochim. Biophys. Acta* **1959**, *34*, 117–123. [CrossRef]
3. Fetzner, S. Ring-Cleaving Dioxygenases with a Cupin Fold. *Appl. Environ. Microbiol.* **2012**, *78*, 2505–2514. [CrossRef] [PubMed]
4. Subbotina, N.M.; Chernykh, A.M.; Taranov, A.I.; Shebanova, A.D.; Moiseeva, O.V.; Ferraroni, M.; Kolomytseva, M.P. Gentisate 1,2-Dioxygenase from the Gram-Positive Bacteria *Rhodococcus opacus* 1CP: Identical Active Sites vs. Different Substrate Selectivities. *Biochimie* **2021**, *180*, 90–103. [CrossRef]
5. Yu, H.; Zhao, S.; Guo, L. Novel Gene Encoding 5-Aminosalicylate 1,2-Dioxygenase from *Comamonas* sp. Strain QT12 and Catalytic Properties of the Purified Enzyme. *J. Bacteriol.* **2018**, *200*, e00395-17. [CrossRef]
6. Adams, M.A.; Singh, V.K.; Keller, B.O.; Jia, Z. Structural and Biochemical Characterization of Gentisate 1,2-Dioxygenase from *Escherichia coli* O157:H7. *Mol. Microbiol.* **2006**, *61*, 1469–1484. [CrossRef]
7. Feng, J.; Che, Y.; Milse, J.; Yin, Y.-J.; Liu, L.; Rückert, C.; Shen, X.-H.; Qi, S.-W.; Kalinowski, J.; Liu, S.-J. The Gene Ncgl2918 Encodes a Novel Maleylpyruvate Isomerase That Needs Mycothiol as Cofactor and Links Mycothiol Biosynthesis and Gentisate Assimilation in *Corynebacterium glutamicum*. *J. Biol. Chem.* **2006**, *281*, 10778–10785. [CrossRef]
8. Di Gennaro, P.; Terreni, P.; Masi, G.; Botti, S.; de Ferra, F.; Bestetti, G. Identification and Characterization of Genes Involved in Naphthalene Degradation in *Rhodococcus opacus* R7. *Appl. Microbiol. Biotechnol.* **2010**, *87*, 297–308. [CrossRef]
9. Grund, E.; Denecke, B.; Eichenlaub, R. Naphthalene Degradation via Salicylate and Gentisate by *Rhodococcus* sp. Strain B4. *Appl. Environ. Microbiol.* **1992**, *58*, 1874–1877. [CrossRef]
10. Jones, D.C.N.; Cooper, R.A. Catabolism of 3-Hydroxybenzoate by the Gentisate Pathway in *Klebsiella pneumoniae* M5a1. *Arch. Microbiol.* **1990**, *154*, 489–495. [CrossRef]
11. Ladd, J.N. Oxidation of Anthranilic Acid by a Species of *Achromobacter* Isolated from Soil. *Nature* **1962**, *194*, 1099–1100. [CrossRef] [PubMed]
12. Liu, T.-T.; Xu, Y.; Liu, H.; Luo, S.; Yin, Y.-J.; Liu, S.-J.; Zhou, N.-Y. Functional Characterization of a Gene Cluster Involved in Gentisate Catabolism in *Rhodococcus* sp. Strain NCIMB 12038. *Appl. Microbiol. Biotechnol.* **2011**, *90*, 671–678. [CrossRef] [PubMed]
13. Liu, T.T.; Zhou, N.Y. Novel L-Cysteine-Dependent Maleylpyruvate Isomerase in the Gentisate Pathway of *Paenibacillus* sp. Strain NyZ101. *J. Bacteriol.* **2012**, *194*, 3987–3994. [CrossRef] [PubMed]
14. Ohmoto, T.; Sakai, K.; Hamada, N.; Ohe, T. Salicylic Acid Metabolism through a Gentisate Pathway by *Pseudomonas* sp. TA-2. *Agric. Biol. Chem.* **1991**, *55*, 1733–1737. [CrossRef]
15. Feng, Y.; Khoo, H.E.; Laa Poh, C.; Poh, C.L. Purification and Characterization of Gentisate 1,2-Dioxygenases from *Pseudomonas alcaligenes* NCIB 9867 and *Pseudomonas putida* NCIB 9869. *Appl. Environ. Microbiol.* **1999**, *65*, 946–950. [CrossRef]
16. Harpel, M.R.; Lipscomb, J.D. Gentisate 1,2-Dioxygenase from *Pseudomonas*. Purification, Characterization, and Comparison of the Enzymes from *Pseudomonas testosteroni* and *Pseudomonas acidovorans*. *J. Biol. Chem.* **1990**, *265*, 6301–6311. [CrossRef]
17. Hirano, S.; Morikawa, M.; Takano, K.; Imanaka, T.; Kanaya, S. Gentisate 1,2-Dioxygenase from *Xanthobacter polyaromaticivorans* 127W. *Biosci. Biotechnol. Biochem.* **2007**, *71*, 192–199. [CrossRef]
18. Werwath, J.; Arfmann, H.A.; Pieper, D.H.; Timmis, K.N.; Wittich, R.M. Biochemical and Genetic Characterization of a Gentisate 1,2-Dioxygenase from *Sphingomonas* sp. Strain RW5. *J. Bacteriol.* **1998**, *180*, 4171–4176. [CrossRef]
19. Liu, D.; Zhu, T.; Fan, L.; Quan, J.; Guo, H.; Ni, J. Identification of a Novel Gentisate 1,2-Dioxygenase from *Silicibacter pomeroyi*. *Biotechnol. Lett.* **2007**, *29*, 1529–1535. [CrossRef]

20. Lee, H.J.; Kim, J.M.; Lee, S.H.; Park, M.; Lee, K.; Madsen, E.L.; Jeon, C.O. Gentisate 1,2-Dioxygenase, in the Third Naphthalene Catabolic Gene Cluster of *Polaromonas naphthalenivorans* CJ2, Has a Role in Naphthalene Degradation. *Microbiology* **2011**, *157*, 2891–2903. [CrossRef]
21. Chen, J.; Li, W.; Wang, M.; Zhu, G.; Liu, D.; Sun, F.; Hao, N.; Li, X.; Rao, Z.; Zhang, X.C. Crystal Structure and Mutagenic Analysis of GDOsp, a Gentisate 1,2-Dioxygenase from *Silicibacter pomeroyi*. *Protein Sci.* **2008**, *17*, 1362–1373. [CrossRef] [PubMed]
22. Liu, D.; Zhu, S.; Ni, J. Purification and Characterisation of a Gentisate 1,2-Dioxygenase from *Ralstonia solanacearum* GMI 1000. *Ann. Microbiol.* **2007**, *57*, 307–312. [CrossRef]
23. Eppinger, E.; Stolz, A. Expansion of the Substrate Range of the Gentisate 1,2-Dioxygenase from *Corynebacterium glutamicum* for the Conversion of Monohydroxylated Benzoates. *Protein Eng. Des. Sel.* **2017**, *30*, 57–65. [CrossRef] [PubMed]
24. Suemori, A.; Kurane, R.; Tomizuka, N. Purification and Properties of Gentisate 1,2-Dioxygenase from *Rhodococcus erythropolis* S-1. *Biosci. Biotechnol. Biochem.* **1993**, *57*, 1781–1783. [CrossRef]
25. Guzik, U.; Hupert-Kocurek, K.; Wojcieszynska, D. Immobilization as a Strategy for Improving Enzyme Properties—Application to Oxidoreductases. *Molecules* **2014**, *19*, 8995–9018. [CrossRef]
26. Rodrigues, R.C.; Berenguer-Murcia, Á.; Carballares, D.; Morellon-Sterling, R.; Fernandez-Lafuente, R. Stabilization of Enzymes via Immobilization: Multipoint Covalent Attachment and Other Stabilization Strategies. *Biotechnol. Adv.* **2021**, *52*, 107821. [CrossRef]
27. Fernandez-Lafuente, R. Stabilization of Multimeric Enzymes: Strategies to Prevent Subunit Dissociation. *Enzym. Microb. Technol.* **2009**, *45*, 405–418. [CrossRef]
28. Bilal, M.; Asgher, M.; Cheng, H.; Yan, Y.; Iqbal, H.M.N. Multi-Point Enzyme Immobilization, Surface Chemistry, and Novel Platforms: A Paradigm Shift in Biocatalyst Design. *Crit. Rev. Biotechnol.* **2019**, *39*, 202–219. [CrossRef]
29. Pessela, B.C.C.; Mateo, C.; Fuentes, M.; Vian, A.; García, J.L.; Carrascosa, A.V.; Guisán, J.M.; Fernández-Lafuente, R. Stabilization of a Multimeric Beta-Galactosidase from *Thermus* sp. Strain T2 by Immobilization on Novel Heterofunctional Epoxy Supports plus Aldehyde-Dextran Cross-Linking. *Biotechnol. Prog.* **2004**, *20*, 388–392. [CrossRef]
30. Arana-Peña, S.; Rios, N.S.; Carballares, D.; Mendez-Sanchez, C.; Lokha, Y.; Gonçalves, L.R.B.; Fernandez-Lafuente, R. Effects of Enzyme Loading and Immobilization Conditions on the Catalytic Features of Lipase From *Pseudomonas fluorescens* Immobilized on Octyl-Agarose Beads. *Front. Bioeng. Biotechnol.* **2020**, *8*, 36. [CrossRef]
31. Mateo, C.; Palomo, J.M.; Fernandez-Lorente, G.; Guisan, J.M.; Fernandez-Lafuente, R. Improvement of Enzyme Activity, Stability and Selectivity via Immobilization Techniques. *Enzym. Microb. Technol.* **2007**, *40*, 1451–1463. [CrossRef]
32. Silva, A.S.; Jacques, R.J.S.; Andreazza, R.; Bento, F.M.; Roesch, L.F.W.; Camargo, F.A.O. Properties of Catechol 1, 2-Dioxygenase in the Cell Free Extract and Immobilized Extract of *Mycobacterium fortuitum*. *Braz. J. Microbiol.* **2013**, *44*, 291–297. [CrossRef] [PubMed]
33. Suma, Y.; Kang, C.S.; Kim, H.S. Noncovalent and Covalent Immobilization of Oxygenase on Single-Walled Carbon Nanotube for Enzymatic Decomposition of Aromatic Hydrocarbon Intermediates. *Environ. Sci. Pollut. Res.* **2016**, *23*, 1015–1024. [CrossRef] [PubMed]
34. Suma, Y.; Lim, H.; Kwean, O.S.; Cho, S.; Yang, J.; Kim, Y.; Kang, C.S.; Kim, H.S. Enzymatic Degradation of Aromatic Hydrocarbon Intermediates Using a Recombinant Dioxygenase Immobilized onto Surfactant-Activated Carbon Nanotube. *Bioresour. Technol.* **2016**, *210*, 117–122. [CrossRef]
35. Das, R.; Hamid, S.B.A.; Annuar, M.S.M. Highly Efficient and Stable Novel NanoBiohybrid Catalyst to Avert 3,4-Dihydroxybenzoic Acid Pollutant in Water. *Sci. Rep.* **2016**, *6*, 33572. [CrossRef]
36. Zhang, L.-S.; Fang, Y.; Zhou, Y.; Ye, B.-C. Improvement of the Stabilization and Activity of Protocatechuate 3,4-Dioxygenase Isolated from *Rhizobium* sp. LMB-1 and Immobilized on Fe_3O_4 Nanoparticles. *Appl. Biochem. Biotechnol.* **2017**, *183*, 1035–1048. [CrossRef]
37. Kwean, O.S.; Cho, S.Y.; Yang, J.W.; Cho, W.; Park, S.; Lim, Y.; Shin, M.C.; Kim, H.S.; Park, J.; Kim, H.S. 4-Chlorophenol Biodegradation Facilitator Composed of Recombinant Multi-Biocatalysts Immobilized onto Montmorillonite. *Bioresour. Technol.* **2018**, *259*, 268–275. [CrossRef]
38. Gkantzou, E.; Chatzikonstantinou, A.V.; Fotiadou, R.; Giannakopoulou, A.; Patila, M.; Stamatis, H. Trends in the Development of Innovative Nanobiocatalysts and Their Application in Biocatalytic Transformations. *Biotechnol. Adv.* **2021**, *51*, 107738. [CrossRef]
39. Garcia-Galan, C.; Berenguer-Murcia, Á.; Fernandez-Lafuente, R.; Rodrigues, R.C. Potential of Different Enzyme Immobilization Strategies to Improve Enzyme Performance. *Adv. Synth. Catal.* **2011**, *353*, 2885–2904. [CrossRef]
40. Giannakopoulou, A.; Patila, M.; Spyrou, K.; Chalmpes, N.; Zarafeta, D.; Skretas, G.; Gournis, D.; Stamatis, H. Development of a Four-Enzyme Magnetic Nanobiocatalyst for Multi-Step Cascade Reactions. *Catalysts* **2019**, *9*, 995. [CrossRef]
41. Yang, J.; Ni, K.; Wei, D.; Ren, Y. One-Step Purification and Immobilization of His-Tagged Protein via Ni^{2+}-Functionalized Fe_3O_4@polydopamine Magnetic Nanoparticles. *Biotechnol. Bioprocess Eng.* **2015**, *20*, 901–907. [CrossRef]
42. Porath, J. Immobilized Metal Ion Affinity Chromatography. *Protein Expr. Purif.* **1992**, *3*, 263–281. [CrossRef]
43. Mateo, C.; Fernández-Lorente, G.; Cortés, E.; Garcia, J.L.; Fernández-Lafuente, R.; Guisan, J.M. One-Step Purification, Covalent Immobilization, and Additional Stabilization of Poly-His-Tagged Proteins Using Novel Heterofunctional Chelate-Epoxy Supports. *Biotechnol. Bioeng.* **2001**, *76*, 269–276. [CrossRef] [PubMed]
44. Lee, J.; Chang, J.H. Facile and High-Efficient Immobilization of Histidine-Tagged Multimeric Protein G on Magnetic Nanoparticles. *Nanoscale Res. Lett.* **2014**, *9*, 664. [CrossRef]

45. Ball, V. Polydopamine Nanomaterials: Recent Advances in Synthesis Methods and Applications. *Front. Bioeng. Biotechnol.* **2018**, *6*, 109. [CrossRef] [PubMed]
46. Liao, J.; Han, S.; Li, X.; He, J.; Secundo, F.; Liang, H. Co-Immobilization of Two-Component Hydroxylase Monooxygenase by Functionalized Magnetic Nanoparticles for Preserving High Catalytic Activity and Enhancing Enzyme Stabilty. *Int. J. Biol. Macromol.* **2020**, *164*, 3163–3170. [CrossRef]
47. Wang, W.; Wang, D.I.C.; Li, Z. Facile Fabrication of Recyclable and Active Nanobiocatalyst: Purification and Immobilization of Enzyme in One Pot with Ni-NTA Functionalized Magnetic Nanoparticle. *Chem. Commun.* **2011**, *47*, 8115–8117. [CrossRef]
48. Sung, H.K.; Jeyakumar, M.; Katzenellenbogen, J.A. Dual-Mode Fluorophore-Doped Nickel Nitrilotriacetic Acid-Modified Silica Nanoparticles Combine Histidine-Tagged Protein Purification with Site-Specific Fluorophore Labeling. *J. Am. Chem. Soc.* **2007**, *129*, 13254–13264. [CrossRef]
49. Yan, Y.; Zheng, Z.; Deng, C.; Zhang, X.; Yang, P. Facile Synthesis of Ti4+-Immobilized Fe_3O_4@polydopamine Core–Shell Microspheres for Highly Selective Enrichment of Phosphopeptides. *Chem. Commun.* **2013**, *49*, 5055. [CrossRef]
50. Kallimanis, A.; Kavakiotis, K.; Perisynakis, A.; Spröer, C.; Pukall, R.; Drainas, C.; Koukkou, A.I. *Arthrobacter phenanthrenivorans* Sp. Nov., to Accommodate the Phenanthrene-Degrading Bacterium *Arthrobacter* sp. Strain Sphe3. *Int. J. Syst. Evol. Microbiol.* **2009**, *59*, 275–279. [CrossRef]
51. Vandera, E.; Kavakiotis, K.; Kallimanis, A.; Kyrpides, N.C.; Drainas, C.; Koukkou, A. Heterologous Expression and Characterization of Two 1-Hydroxy-2-Naphthoic Acid Dioxygenases from *Arthrobacter phenanthrenivorans*. *Appl. Environ. Microbiol.* **2012**, *78*, 621–627. [CrossRef] [PubMed]
52. Tsagogiannis, E.; Vandera, E.; Primikyri, A.; Asimakoula, S.; Tzakos, A.G.; Gerothanassis, I.P.; Koukkou, A.-I. Characterization of Protocatechuate 4,5-Dioxygenase from *Pseudarthrobacter phenanthrenivorans* Sphe3 and In Situ Reaction Monitoring in the NMR Tube. *Int. J. Mol. Sci.* **2021**, *22*, 9647. [CrossRef] [PubMed]
53. Bradford, M.M. A Rapid and Sensitive Method for the Quantitation of Microgram Quantities of Protein Utilizing the Principle of Protein-Dye Binding. *Anal. Biochem.* **1976**, *72*, 248–254. [CrossRef]
54. William, S.; Feil, H.; Copeland, A. Bacterial Genomic DNA Isolation Using CTAB. *Sigma* **2012**, *50*, 6876.
55. Hanahan, D. Studies on Transformation of *Escherichia coli* with Plasmids. *J. Mol. Biol.* **1983**, *166*, 557–580. [CrossRef]
56. Chung, C.T.; Miller, R.H. A Rapid and Convenient Method for the Preparation and Storage of Competent Bacterial Cells. *Nucleic Acids Res.* **1988**, *16*, 3580. [CrossRef]
57. Altschul, S. Gapped BLAST and PSI-BLAST: A New Generation of Protein Database Search Programs. *Nucleic Acids Res.* **1997**, *25*, 3389–3402. [CrossRef]
58. Thompson, J.D.; Higgins, D.G.; Gibson, T.J. CLUSTAL W: Improving the Sensitivity of Progressive Multiple Sequence Alignment through Sequence Weighting, Position-Specific Gap Penalties and Weight Matrix Choice. *Nucleic Acids Res.* **1994**, *22*, 4673. [CrossRef]
59. Kumar, S.; Stecher, G.; Tamura, K. MEGA7: Molecular Evolutionary Genetics Analysis Version 7.0 for Bigger Datasets. *Mol. Biol. Evol.* **2016**, *33*, 1870–1874. [CrossRef]
60. Sambrook, J.F.; Russell, D.W. *Molecular Cloning: A Laboratory Manual*, 3rd ed.; Cold Spring Harbor Laboratory Press: New York, NY, USA, 2003; Volumes 1–3.
61. Boudrant, J.; Woodley, J.M.; Fernandez-Lafuente, R. Parameters Necessary to Define an Immobilized Enzyme Preparation. *Process Biochem.* **2020**, *90*, 66–80. [CrossRef]
62. Dias Gomes, M.; Woodley, J.M. Considerations When Measuring Biocatalyst Performance. *Molecules* **2019**, *24*, 3573. [CrossRef] [PubMed]
63. Saitou, N.; Nei, M. The Neighbor-Joining Method: A New Method for Reconstructing Phylogenetic Trees. *Mol. Biol. Evol.* **1987**, *4*, 406–425. [CrossRef] [PubMed]
64. Suárez, M.; Ferrer, E.; Martín, M. Purification and Biochemical Characterization of Gentisate 1,2-Dioxygenase from *Klebsiella pneumoniae* M5a1. *FEMS Microbiol. Lett.* **1996**, *143*, 89–95. [CrossRef]
65. Kiemer, P.; Tshisuaka, B.; Fetzner, S.; Lingens, F. Degradation of Benzoate via Benzoyl-Coenzyme A and Gentisate by *Bacillus stearothermophilus* PK1, and Purification of Gentisate 1,2-Dioxygenase. *Biol. Fertil. Soils* **1996**, *23*, 307–313. [CrossRef]
66. Kotake, T.; Matsuzawa, J.; Suzuki-Minakuchi, C.; Okada, K.; Nojiri, H.; Iwata, K. Purification and Partial Characterization of the Extradiol Dioxygenase, 2′-Carboxy-2,3-Dihydroxybiphenyl 1,2-Dioxygenase, in the Fluorene Degradation Pathway from *Rhodococcus* sp. Strain DFA3. *Biosci. Biotechnol. Biochem.* **2016**, *80*, 719–725. [CrossRef] [PubMed]
67. Harpel, M.R.; Lipscomb, J.D. Gentisate 1,2-Dioxygenase from *Pseudomonas*. Substrate Coordination to Active Site Fe^{2+} and Mechanism of Turnover. *J. Biol. Chem.* **1990**, *265*, 22187–22196. [CrossRef]
68. Yeo, C.C.; Tan, C.L.; Gao, X.; Zhao, B.; Poh, C.L. Characterization of HbzE-Encoded Gentisate 1,2-Dioxygenase from *Pseudomonas alcaligenes* NCIMB 9867. *Res. Microbiol.* **2007**, *158*, 608–616. [CrossRef]
69. Huang, L.; Hu, H.; Tang, H.; Liu, Y.; Xu, P.; Shi, J.; Lin, K.; Luo, Q.; Cui, C.; Luo, S.; et al. Identification and Characterization of a Novel Gentisate 1,2-Dioxygenase Gene from a Halophilic *Martelella* Strain. *Sci. Rep.* **2015**, *5*, 14307. [CrossRef]
70. Guzik, U.; Hupert-Kocurek, K.; Krysiak, M.; Wojcieszyńska, D. Degradation Potential of Protocatechuate 3,4-Dioxygenase from Crude Extract of *Stenotrophomonas maltophilia* Strain KB2 Immobilized in Calcium Alginate Hydrogels and on Glyoxyl Agarose. *Biomed. Res. Int.* **2014**, *2014*, 138768. [CrossRef]

71. Barry, K.P.; Taylor, E.A. Characterizing the Promiscuity of LigAB, a Lignin Catabolite Degrading Extradiol Dioxygenase from *Sphingomonas paucimobilis* SYK-6. *Biochemistry* **2013**, *52*, 6724–6736. [CrossRef]
72. Ha, E.J.; Kim, B.S.; Park, E.K.; Song, K.W.; Lee, S.G.; An, S.S.A.; Paik, H.-j. Site-Specific Reversible Immobilization and Purification of His-Tagged Protein on Poly(2-Acetamidoacrylic Acid) Hydrogel Beads. *Polym. Adv. Technol.* **2013**, *24*, 75–80. [CrossRef]
73. Vahidi, A.K.; Yang, Y.; Ngo, T.P.N.; Li, Z. Simple and Efficient Immobilization of Extracellular His-Tagged Enzyme Directly from Cell Culture Supernatant as Active and Recyclable Nanobiocatalyst: High-Performance Production of Biodiesel from Waste Grease. *ACS Catal.* **2015**, *5*, 3157–3161. [CrossRef]
74. Zhou, L.J.; Li, R.F.; Li, X.Y.; Zhang, Y.W. One-step Selective Affinity Purification and Immobilization of His-tagged Enzyme by Recyclable Magnetic Nanoparticles. *Eng. Life Sci.* **2021**, *21*, 364. [CrossRef] [PubMed]
75. Bilal, M.; Zhao, Y.; Rasheed, T.; Iqbal, H.M.N. Magnetic Nanoparticles as Versatile Carriers for Enzymes Immobilization: A Review. *Int. J. Biol. Macromol.* **2018**, *120*, 2530–2544. [CrossRef] [PubMed]
76. Giannakopoulou, A.; Chatzikonstantinou, A.V.; Chalmpes, N.; Tsapara, G.; Gournis, D.; Polydera, A.C.; Stamatis, H. Development of a Novel Bi-Enzymatic Nanobiocatalyst for the Efficient Bioconversion of Oleuropein to Hydroxytyrosol. *Catalysts* **2021**, *11*, 749. [CrossRef]
77. Pathmamanoharan, C.; Wijkens, P.; Grove, D.M.; Philipse, A.P. Paramagnetic Silica Particles: Synthesis and Grafting of a Silane Coupling Agent Containing Nickel Ions onto Colloidal Silica Particles. *Langmuir* **1996**, *12*, 4372–4377. [CrossRef]
78. Ji, Y.; Yang, X.; Ji, Z.; Zhu, L.; Ma, N.; Chen, D.; Jia, X.; Tang, J.; Cao, Y. DFT-Calculated IR Spectrum Amide I, II, and III Band Contributions of N -Methylacetamide Fine Components. *ACS Omega* **2020**, *5*, 8572–8578. [CrossRef]
79. Wishart, D.S.; Knox, C.; Guo, A.C.; Eisner, R.; Young, N.; Gautam, B.; Hau, D.D.; Psychogios, N.; Dong, E.; Bouatra, S.; et al. HMDB: A Knowledgebase for the Human Metabolome. *Nucleic Acids Res.* **2009**, *37*, D603–D610. [CrossRef]
80. Jiao, M.; He, J.; Sun, S.; Vriesekoop, F.; Yuan, Q.; Liu, Y.; Liang, H. Fast Immobilization of Human Carbonic Anhydrase II on Ni-Based Metal-Organic Framework Nanorods with High Catalytic Performance. *Catalysts* **2020**, *10*, 401. [CrossRef]
81. Zhang, C.; Luo, S.; Chen, W. Activity of Catalase Adsorbed to Carbon Nanotubes: Effects of Carbon Nanotube Surface Properties. *Talanta* **2013**, *113*, 142–147. [CrossRef]
82. Di Nardo, G.; Roggero, C.; Campolongo, S.; Valetti, F.; Trotta, F.; Gilardi, G. Catalytic Properties of Catechol 1,2-Dioxygenase from *Acinetobacter radioresistens* S13 Immobilized on Nanosponges. *Dalt. Trans.* **2009**, *2*, 6507. [CrossRef] [PubMed]
83. Verma, M.L.; Chaudhary, R.; Tsuzuki, T.; Barrow, C.J.; Puri, M. Immobilization of β-Glucosidase on a Magnetic Nanoparticle Improves Thermostability: Application in Cellobiose Hydrolysis. *Bioresour. Technol.* **2013**, *135*, 2–6. [CrossRef] [PubMed]
84. Zhou, Y.; Yuan, S.; Liu, Q.; Yan, D.; Wang, Y.; Gao, L.; Han, J.; Shi, H. Synchronized Purification and Immobilization of His-Tagged β-Glucosidase via Fe_3O_4/PMG Core/Shell Magnetic Nanoparticles. *Sci. Rep.* **2017**, *7*, 41741. [CrossRef] [PubMed]
85. Alemzadeh, I.; Nejati, S. Phenols Removal by Immobilized Horseradish Peroxidase. *J. Hazard. Mater.* **2009**, *166*, 1082–1086. [CrossRef] [PubMed]
86. Schnell, S.; Hanson, S.M. A Test for Measuring the Effects of Enzyme Inactivation. *Biophys. Chem.* **2007**, *125*, 269–274. [CrossRef]
87. Kalogeris, E.; Sanakis, Y.; Mamma, D.; Christakopoulos, P.; Kekos, D.; Stamatis, H. Properties of Catechol 1,2-Dioxygenase from *Pseudomonas putida* Immobilized in Calcium Alginate Hydrogels. *Enzyme Microb. Technol.* **2006**, *39*, 1113–1121. [CrossRef]
88. Wojcieszyńska, D.; Hupert-Kocurek, K.; Jankowska, A.; Guzik, U. Properties of Catechol 2,3-Dioxygenase from Crude Extract of *Stenotrophomonas maltophilia* Strain KB2 Immobilized in Calcium Alginate Hydrogels. *Biochem. Eng. J.* **2012**, *66*, 1–7. [CrossRef]
89. Verma, M.L.; Barrow, C.J.; Kennedy, J.F.; Puri, M. Immobilization of β-d-Galactosidase from *Kluyveromyces lactis* on Functionalized Silicon Dioxide Nanoparticles: Characterization and Lactose Hydrolysis. *Int. J. Biol. Macromol.* **2012**, *50*, 432–437. [CrossRef]
90. Darwesh, O.M.; Matter, I.A.; Eida, M.F. Development of Peroxidase Enzyme Immobilized Magnetic Nanoparticles for Bioremediation of Textile Wastewater Dye. *J. Environ. Chem. Eng.* **2019**, *7*, 102805. [CrossRef]